

Combined Effect of Co and W on Deformation Resistance of 12Cr Heat-Resistant Steel for USC Steam Turbines

Huiran Cui, Feng Sun, Ke Chen, and Jiansheng Wu

(Submitted May 4, 2010; in revised form October 1, 2010)

12Cr heat-resistant steels with different concentrations of Co and W, with Mo equivalent (Mo + 1/2W) fixed at 1.6 wt.%, were prepared by arc-melting and hot rolling processes. Mechanical properties were evaluated by tensile tests conducted at a low strain rate $2 \times 10^{-5} \text{ s}^{-1}$ at 575, 600, and 625 °C. Microstructure of the steels was investigated via optical microscopy (OM) and electron transmission microscopy (TEM). The results show that when the content of W is fixed, the steel with 3.1 wt.% Co and the steel with 3.8 wt.% Co are found to obtain the best deformation resistance values at 575, 600, and at 625 °C; when the Co content is fixed, the steel with 1.5 wt.% W shows better performance. The highest ultimate tensile strength (UTS) and yield stress (YS) were achieved for the steel when its W content is at 1.5 wt.% and Co content is at 3.1 wt.% or 3.8 wt.%. Deformation resistance is related to the initial dislocation density in the steels, which increases with increasing Co content and decreases with increasing W content. It is verified that the deformation mechanism of the tested steels during high-temperature tensile tests at a low strain rate is that of the recovery-controlled dislocation creep. Furthermore, the thermodynamic calculation result is in agreement with the experimental result, demonstrating that 0.85Mo-1.5W-3.8Co steel has the best deformation resistance at 625 °C. Therefore, 0.85Mo-1.5W-3.1Co steel is recommended as a potential candidate material for 600 °C class steam turbines, and 0.85Mo-1.5W-3.8Co steel is also a potential material for 625 °C class Ultra supercritical (USC) steam turbines.

Keywords Co, deformation resistance, USC steam turbines, W, 12Cr heat-resistant steel

1. Introduction

Ultra supercritical (USC) power plants hold the promising potential with higher efficiencies and lower emissions of CO₂ (Ref 1-3). Because the efficiency of fossil power plants is a strong function of steam temperature and pressure, there is a further incentive to raise the steam turbine inlet temperature from current level of 600-625 °C, perhaps up to 650 °C (Ref 1-5). 9-12% Cr (all the elemental contents in this article are presented in wt.%) martensite/ferrite steel is recognized as a key material used for USC power plant components, because it has a high thermal conductivity and a low thermal expansion coefficient, and is less susceptible to the thermal fatigue than the austenitic stainless steel (Ref 5).

Development of 9-12% Cr steels has been based traditionally on trial and error via creep testing of a large number of tested alloys, and it is costly and time-consuming. Thus, short-term test methods for accurately assessing the creep life of the steels is badly required, and many have been proposed (Ref 6). The constant strain rate method, which is originally proposed by Rajakovics (Ref 6), is to extrapolate creep rate based on the fact that the creep deformation and the deformation in low

constant strain rate tensile tests share a same deformation mechanism, which is recovery-controlled dislocation creep (Ref 7). Using this method, Frank et al. (Ref 8) obtained very promising results on power station components, and Steen also has successfully assessed the creep life of a number of high temperature materials (Ref 9). However, in the above mentioned studies, a series of complex mathematical reasoning must be dealt with to determine the steady-state creep rate at a given stress or the creep stress for a given creep rate.

In this article, a more intuitive description method is provided to predict creep resistance of 9-12% Cr steels through low strain rate tensile testing, in which the dislocation creep is characterized by behavior of strain hardening and strain softening in low strain rate tensile testing. Stronger strain hardening or slower strain softening indicates that the process of dislocation recovery and recrystallization is retarded. Accordingly, material with higher strain hardening and slower strain softening is believed to possess stronger deformation resistance.

In this study, mechanical properties for the tested steels were evaluated by high-temperature tensile tests conducted with lower strain rate $2 \times 10^{-5} \text{ s}^{-1}$ at 575, 600, and 625 °C, to investigate the deformation resistance of the 12Cr heat-resistant steels in which the contents of W and Co were systematically changing. The effect of W and Co on the deformation resistance was focused on, and alloy design of Co/W-strengthened 12Cr heat-resistant steels for USC steam turbines was conducted.

2. Experimental Procedure

Nominal compositions of 12Cr heat-resistant steels with different concentration of Co and W, while Mo equivalent

Huiran Cui, Feng Sun, Ke Chen, and Jiansheng Wu, School of Materials Science and Engineering, Shanghai Jiao Tong University, Shanghai 200240, China. Contact e-mails: chr2005@sjtu.edu.cn, fsun@sjtu.edu.cn, chenke83@gmail.com, and wujs@sjtu.edu.cn.

Table 1 Nominal composition (wt.%) of the designed alloys

Alloys	C	Cr	N	Ni	V	Nb	Si	Mn	Mo	W	Co
1.6Mo-0W-2.4Co	0.125	10.35	0.03	0.22	0.2	0.08	0.115	0.2	1.6	0	2.4
1.6Mo-0W-3.1Co	0.125	10.35	0.03	0.22	0.2	0.08	0.115	0.2	1.6	0	3.1
1.6Mo-0W-3.8Co	0.125	10.35	0.03	0.22	0.2	0.08	0.115	0.2	1.6	0	3.8
0.85Mo-1.5W-2.4Co	0.125	10.35	0.03	0.22	0.2	0.08	0.115	0.2	0.85	1.5	2.4
0.85Mo-1.5W-3.1Co	0.125	10.35	0.03	0.22	0.2	0.08	0.115	0.2	0.85	1.5	3.1
0.85Mo-1.5W-3.8Co	0.125	10.35	0.03	0.22	0.2	0.08	0.115	0.2	0.85	1.5	3.8
0.1Mo-3W-2.4Co	0.125	10.35	0.03	0.22	0.2	0.08	0.115	0.2	0.1	3	2.4
0.1Mo-3W-3.1Co	0.125	10.35	0.03	0.22	0.2	0.08	0.115	0.2	0.1	3	3.1
0.1Mo-3W-3.8Co	0.125	10.35	0.03	0.22	0.2	0.08	0.115	0.2	0.1	3	3.8

(Mo + 1/2W) was fixed at 1.6%, are shown in Table 1, and the measured compositions by chemical composition analysis were found to be in good agreement with the nominal ones. The alloys were prepared by arc-melting to the ingots of 80 g. These ingots were hot rolled at 1100 °C to about 2.5 mm thick, then austenitized at 1120 °C for 1 h (quenched in oil), and finished by tempering at 680 °C for 2 h.

Specimens for flat tensile tests (10-mm gauge length, 4-mm width and 2-mm thickness) were prepared by machining from the as-tempered plates. The tensile tests were performed in air using a SHIMAZU AG-100KNA test machine equipped with a three-zone resistance furnace under the strain rate $2 \times 10^{-5} \text{ s}^{-1}$ at 575, 600, and 625 °C. Specimens were held at test temperature for 15 min after about 45 min of heating up to desired temperature, and air-cooled after fracture. Tensile direction was parallel to the rolling direction. Tensile displacements were measured using an extensometer attached to the gauge portion of the specimen.

Microstructure of the tested steels was observed by OM (Leica DMRD) and TEM (JSM-2010) operating at 200 kV.

JMatPro was used to predict the formation of different phases at different compositions, based on CALPHAD (calculation of phase diagrams) that requires mathematical description of thermodynamics of the system of interest. The described thermodynamic properties of the phases in the system are then input into application software to calculate phase equilibria by Gibbs energy minimization process (Ref 10).

3. Results and Discussion

3.1 Mechanical Properties

3.1.1 Effects of Co and W on Deformation Resistance.

Figures 1-3 present the strain-hardening rates ($d\sigma/d\varepsilon_p$) versus plastic strain curves of three kinds of steel with fixed W contents, respectively of 0, 1.5, and 3% at the given temperatures. It is obvious that the trends of strain-hardening rates are similar to each other for all the tested steels at the three temperatures, that is, the strain-hardening curves all display a three-stage hardening behavior: strain-hardening stage, quasi-steady stage, and strain-softening stage. The initial strain-hardening stage is one, where very high strain-hardening rates are found at the onset of the deformation, but the strain-hardening rates immediately afterward decrease rapidly with strain in the plastic strain range from 0 to 0.05. The ending one is weakening of the hardening trend (strain-softening) stage; it is also apparent that the strain-hardening rate in this stage again drops rapidly due to geometrical softening caused by necking

(Ref 11). Thus, there was a quasi-steady state in the strain range around 0.05-0.13 between the hardening stage and the softening stage. Moreover, the average strain-hardening rate seemed to be higher at lower temperatures and the stage of strain hardening is broadened with increasing temperature, and the length of the softening stage is longer with decreasing temperature.

As shown in Fig. 1(a) and (b), the strain hardening rate of 1.6Mo-0W-3.1Co steel is the highest and its length of the softening stage is longer at 575 and 600 °C. However, the strain-hardening rate of the steel without W and with 3.8% Co (1.6Mo-0W-3.8Co) is higher than those of the other W free alloys and the softening trend is slower at 625 °C (in Fig. 1c). As indicated in Fig. 2, the average strain-hardening rate of the steel containing 1.5% W and 3.1% Co is the highest at 575 and 600 °C. Nevertheless, the steel with 1.5% W and 3.1% Co shows higher strain-hardening rate and broadening of the strain-softening region than the other two steels at 625 °C. As a result, when W with fixed content of 1.5% combines with the steel having 3.1% Co and the steel with 3.8% Co, the former is supposed to show the best deformation resistance property at lower temperatures (575 and 600 °C) and the latter at higher temperature (625 °C), respectively. In Fig. 3, the overall strain-hardening rate of the high W steel with 3.8% Co is higher than those of the other steel at 575 °C (Fig. 3a). However, the Co content dependencies of $d\sigma/d\varepsilon_p$ versus ε_p curves of the high W steel appear to be less sensitive to Co content at 600 °C (Fig. 3b). At 625 °C, the strain-hardening rate decreases with increasing Co content (Fig. 3c). Consequently, the high W steel with 3.8% Co obtains the better performance at lower temperature, but the steel with lower Co content shows the stronger deformation resistance at higher temperature.

As is well known, the steel with stronger work hardening (higher strain-hardening rate or longer hardening stage) or slower strain softening (lower decreasing rate or longer softening stage) obtains better deformation resistance under the same conditions, when oxidation and material inhomogeneity are disregarded. The analysis methods for the effect of W on the deformation resistance are similar to those of effect of Co on the deformation resistance above. The results of optimization of Co and W in the studied steels obtaining best performance are listed in Table 2. It is clear that when W content is fixed, Co content set at 3.1% is preferred at 575 and 600 °C, but at 625 °C, Co content at 3.8% is better. Further, when Co content is fixed, W content set at 1.5% is the optimized value of the W content for the designed steels at the three temperatures. Therefore, 0.85Mo-1.5W-3.1Co steel is suitable for 12Cr ferrite heat-resistant steels for USC steam turbine in which the steam temperature is in the range of 575-600 °C. However, 0.85Mo-1.5W-3.8Co steel can be used at 625 °C level.

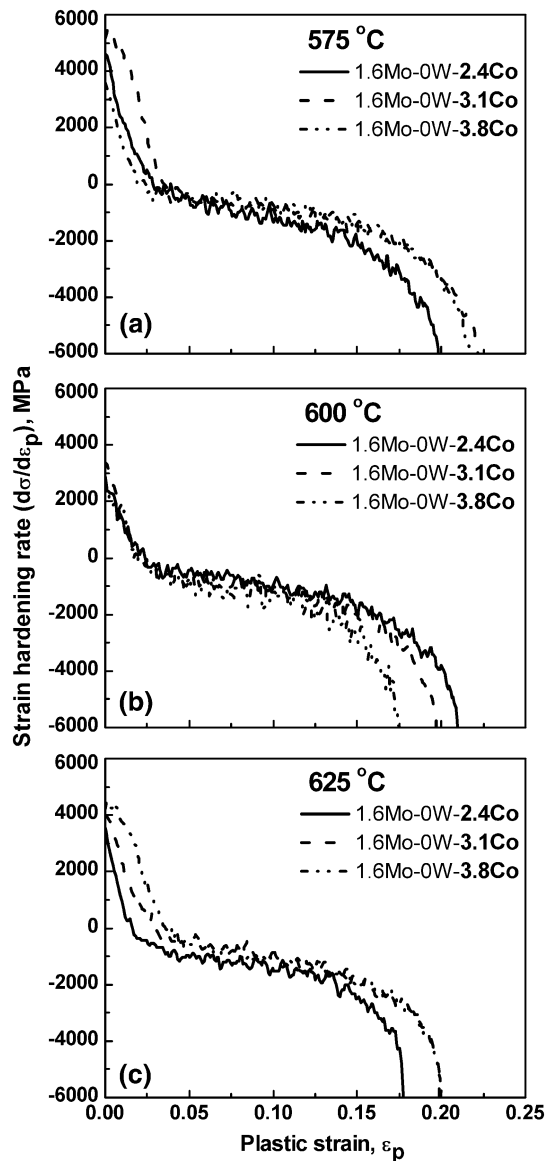


Fig. 1 The strain-hardening rate-plastic strain curves of W-free steels with different Co content at (a) 575 °C, (b) 600 °C, and (c) 625 °C

3.1.2 UTS and YS. The effects of Co content and W content on UTS and YS are presented in Fig. 4 and 5, respectively. Both UTS and YS increase with decreasing temperature. As shown in Fig. 4(a) and 5(a), UTS increases with increasing Co content and changes little while varying the W content at 575 °C; however, UTS changes little while varying the Co content at 600 °C and 625 °C and increases with increasing W content at 625 °C. An interesting point is that UTS values of the steel with 1.5% W and 3.1% Co are the highest at 600 and 625 °C, and UTS values of the steel containing 1.5% W and 3.8% Co are slightly lower than those of the steel with 1.5% W and 3.1% Co. However, UTS values of these two steels are higher than those of the other steels. Accordingly, they are suggested to have better performance at 600 and 625 °C.

Figures 4(b) and 5(b) show that YS varies with Co content and W content. As shown in Fig. 4(b), the steels containing 3.1% Co show the highest yield strength at 600 and 625 °C for

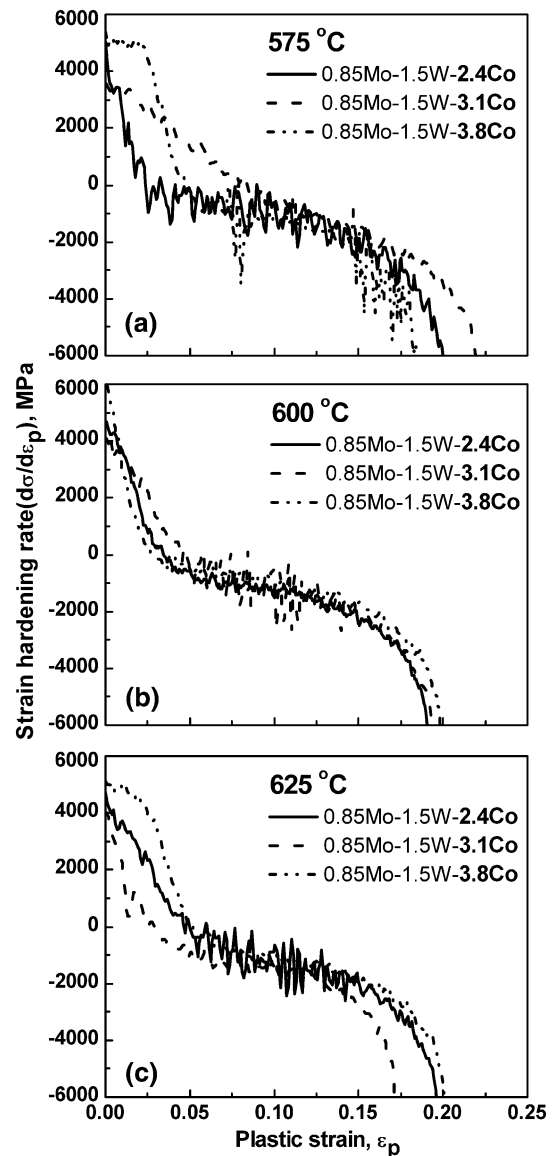


Fig. 2 The strain-hardening rate-plastic strain curves of 1.5% W steels with different Co content at (a) 575 °C, (b) 600 °C, and (c) 625 °C

W free steels and 1.5% W steels, and YS of the steels with 3% W increases rapidly with increasing Co content. In Fig. 5(b), YS decreases with increasing W content from 0 to 1.5%, and then increases with increasing W content from 1.5 to 3% at 575 °C. The steel with 1.5% W has the highest YS at 600 °C, but YS of W-free steel is the highest at 625 °C. Consequently, when the W content is lower (0% or 1.5%), the Co content set at 3.1% is preferred at 600 °C or 625 °C, while for high W (3%) steel, the more the Co content, the higher the YS is. The above results are basically in accordance with the results based on the analysis of strain-hardening behavior listed in Table 2.

3.2 Microstructure

Figure 6 shows the optical micrographs of the tempered steels. It is clear that the tested steels represent typical tempered lath martensite structure in the entire volume. Prior austenite grain size increases with Co content but barely changes with W content, as shown in Fig. 6.

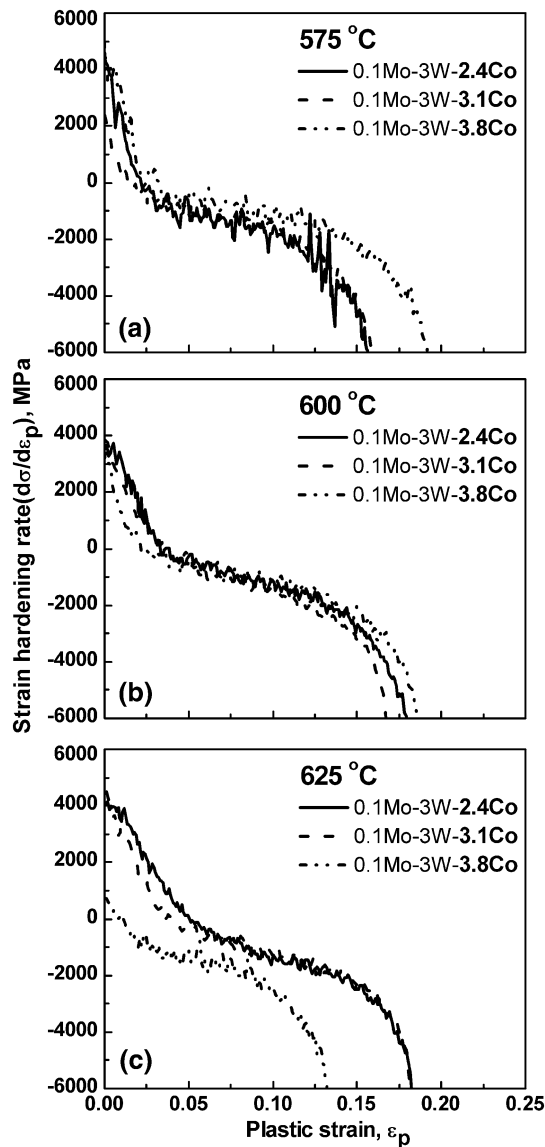


Fig. 3 The strain-hardening rate-plastic strain curves of 3% W steels with different Co content at (a) 575 °C, (b) 600 °C, and (c) 625 °C

Table 2 The results of optimization of Co and W for alloy design

	575 °C	600 °C	625 °C
0 W	3.1% Co	3.1% Co	3.8% Co
1.5% W	3.1% Co	3.1% Co	3.8% Co
3% W	3.8% Co	3.1% Co	2.4% Co
2.4% Co	1.5% W	0 W	1.5% W
3.1% Co	1.5% W	1.5% W	0 W
3.8% Co	1.5% W	1.5% W	1.5% W

There are several factors known to affect the YS of a material. One of them is the grain size. According to the well-known Hall-Petch relationship, YS increases with decrease in grain size. It is obvious that this cannot provide an explanation for the increase of YS between 2.4 and 3.1% Co steels.

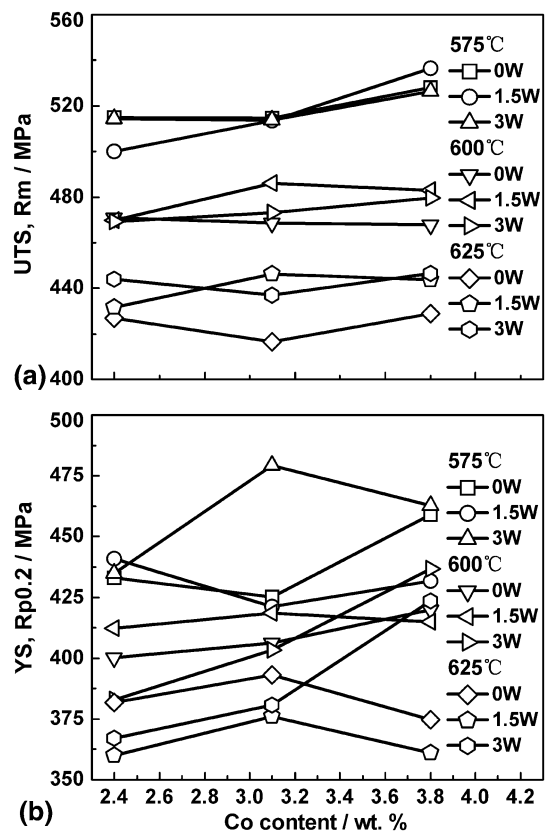


Fig. 4 Engineering strength changes with Co content: (a) UTS and (b) YS

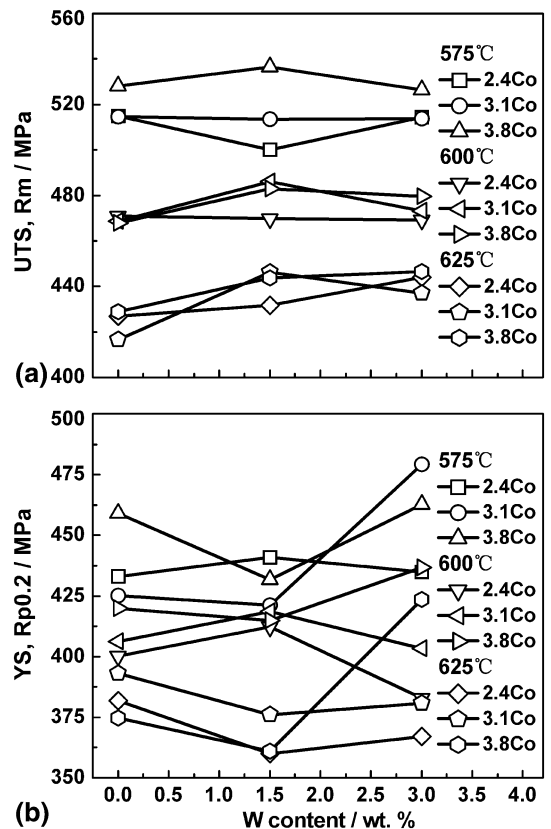


Fig. 5 Engineering strength changes with W content: (a) UTS and (b) YS

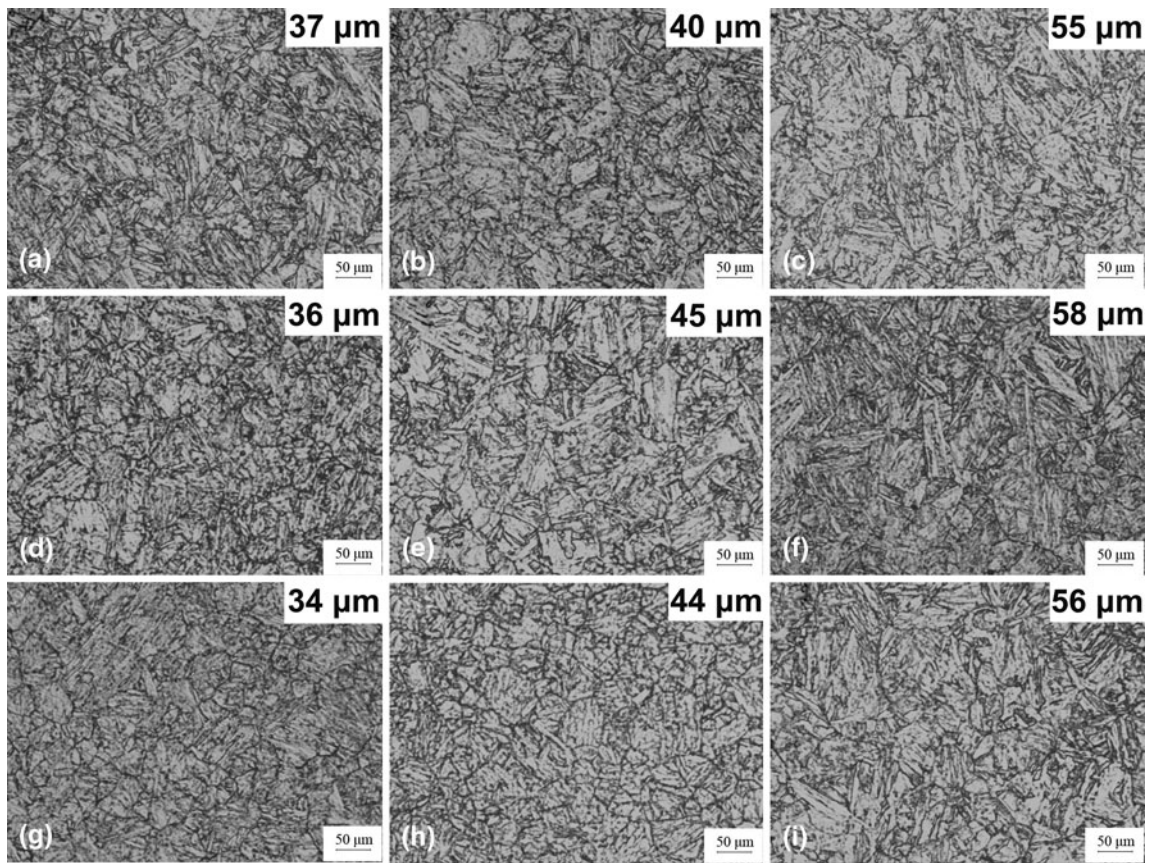


Fig. 6 Optical micrographs of the tested steels

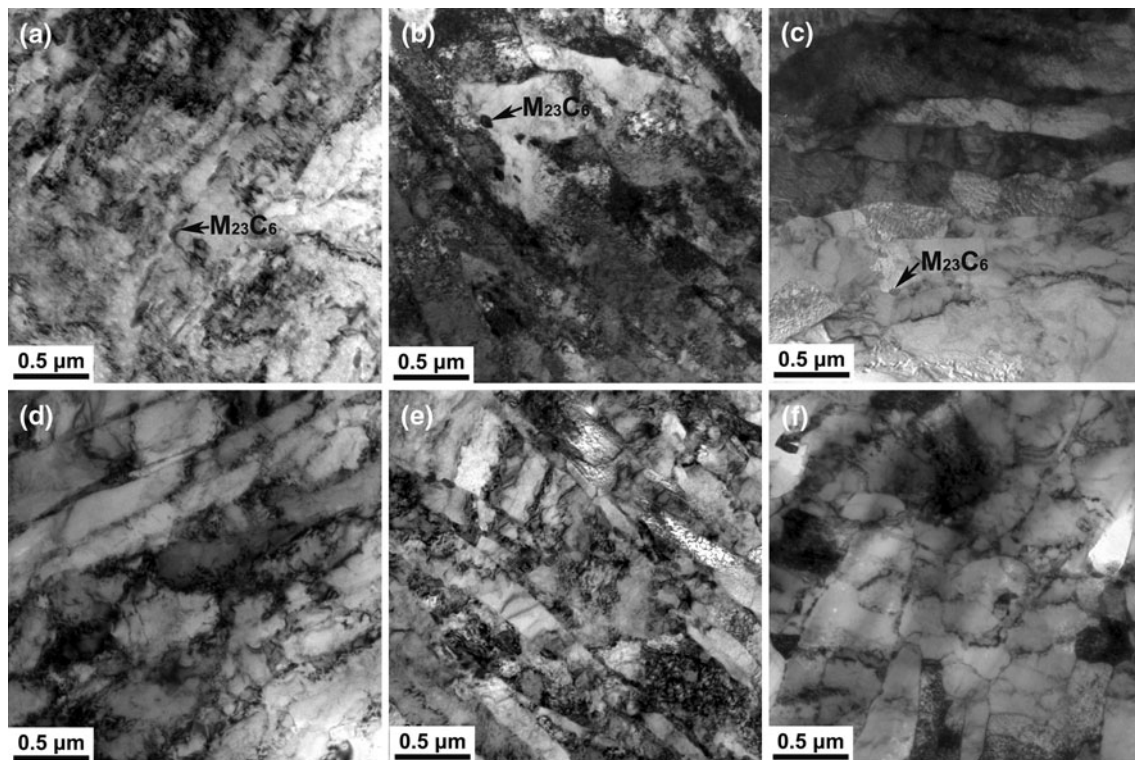


Fig. 7 TEM micrographs of the tested steels before and after tensile testing at 625 °C: (a) 0.85Mo-1.5W-3.1Co, as-tempered, (b) 0.85Mo-1.5W-3.8Co, as-tempered, (c) 0.1Mo-3W-3.8Co, as-tempered, (d) 0.85Mo-1.5W-3.1Co, after testing, (e) 0.85Mo-1.5W-3.8Co, after testing, and (f) 0.1Mo-3W-3.8Co, after testing

However, increase in grain size contributes to the significant decrease in YS with increase in Co addition from 3.1 to 3.8% in the low W (0% or 1.5%) steels.

Figure 7(a)-(c) give TEM micrographs of 0.85Mo-1.5W-3.1Co, 0.85Mo-1.5W-3.8Co, and 0.1Mo-3W-3.8Co steels in the as-tempered condition, and the corresponding TEM images of the steels after tensile testing at 625 °C are shown in Fig. 7(d)-(f). In the as-tempered condition (Fig. 7a-c), the tested steels are characterized by fine lath boundaries with a high density of free dislocations within the subgrains. $M_{23}C_6$ carbides have been extensively observed to locate along former austenite grain boundaries and martensite lath boundaries. Fine precipitates identified as MX carbonitrides with high density have been observed inside grains. However, the initial dislocation density within the sub-grains increases with increasing Co content or decreasing W content. Dislocation density in 0.85Mo-1.5W-3.8Co steel is a little higher than that in 0.85Mo-1.5W-3.1Co steel, and in both these steels, it is much higher than that in the 0.1Mo-3W-3.8Co steel. Experimental results indicate that deformation resistance of 0.85Mo-1.5W-3.8Co steel at 625 °C is better than that of 0.85Mo-1.5W-3.1Co (Fig. 3c) and 0.1Mo-3W-3.8Co steels, which are probably connected with its higher dislocation density. Creep rupture strength of the 9-12% Cr steels with high initial dislocation density was found to be much higher than that of the steels with low dislocation density, and the high density of dislocations make a considerable contribution to the creep rupture strength of the 9% Cr steels (Ref 12).

In Fig. 7(d)-(f), recovery of martensite lath structure of as-tempered condition to a realignment of subgrains and growth of subgrains after tensile testing at 625 °C can be observed. Therefore, the deformation mechanism of the tested steels during high-temperature tensile tests with low strain rate is dislocation creep controlled by recovery, which is in accordance with the creep deformation mechanism for creep tests. It is also obvious that 0.85Mo-1.5W-3.8Co steel shows less recovery compared to the other ones, which may be related to its higher dislocation density, and this is in good agreement with the results from low strain rate tensile testing. As for the precipitates, no new phase has been detected, and no coarsening occurs for both $M_{23}C_6$ carbides and MX carbonitrides after the tensile tests.

3.3 Thermodynamics Calculation

The high creep resistance of 9-12% Cr ferritic heat-resistant steels is mainly attributed to precipitation hardening of $M_{23}C_6$ carbides and MX carbonitrides for maintaining the microstructural stability, and partly to solid-solution hardening of W and Mo, etc. (Ref 13). The degradation of creep properties of the steel during long-term exposure is generally accompanied by ripening of $M_{23}C_6$ carbides and precipitation of new phase such as Laves phase and Z phase.

The equilibrium mole fraction of the second phases ($M_{23}C_6$, MX and Laves phase) in tested steels at 625 °C changing with Co content calculated with thermodynamic JMatPro software is shown in Fig. 8. As displayed in Fig. 8(a), $M_{23}C_6$ carbides increase with increasing Co content but decrease with increasing W content. Amount of $M_{23}C_6$ carbides of the steel with 1.5% W is only slightly lower than that of the W-free steel, but is much higher than that of the steels containing 3% W. To form more $M_{23}C_6$ precipitates, the W content is set at 0 W or 1.5% W, and the Co content is set at 3.8%.

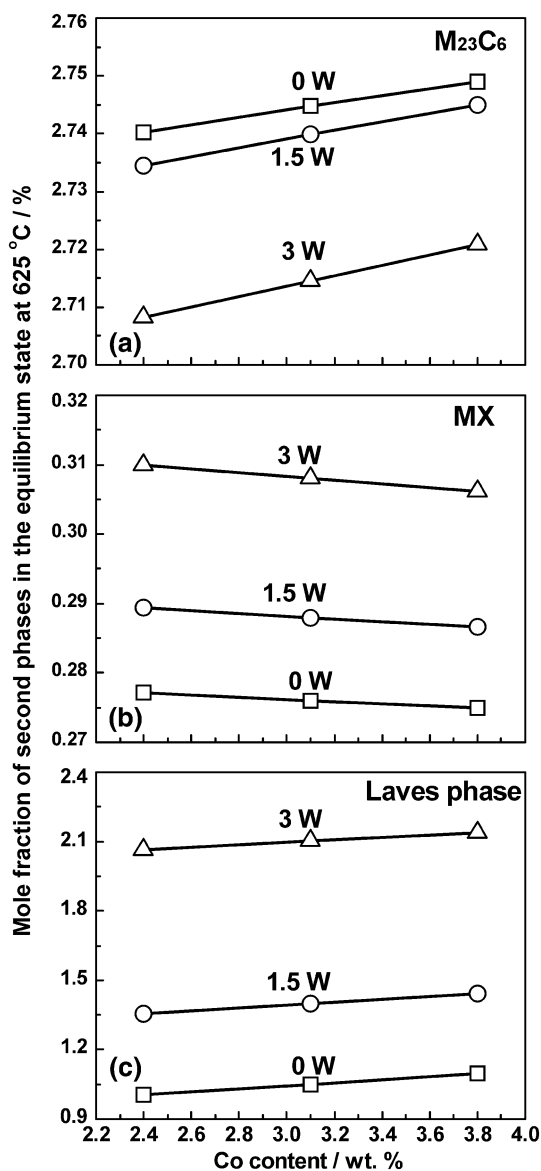


Fig. 8 The equilibrium mole fraction of second phases in the tested steels at 625 °C varying with Co content: (a) $M_{23}C_6$, (b) MX, and (c) Laves phase

The amount of MX precipitates declines slightly when changing the Co content from 2.4 to 3.8%, and increases with increasing W content (Fig. 8b). In Fig. 8(c), Laves phase also barely changes with Co content, but increases significantly with increasing W content. For the discussed steels, the 3% W steels can precipitate more MX carbonitrides at 625 °C. Unfortunately, the amount of $M_{23}C_6$ of the high W steels is a lot less than that of the other steels, and mole fraction of Laves phase in the 3% W steels is much more than the other steels, which may be detrimental for the creep strength of the high W steels because the precipitation of Laves phase promotes the depletion of Mo and W from solid solution (Ref 14). Therefore, to ensure the high amount of $M_{23}C_6$ and MX, and to decrease the volume fraction of the harmful Laves phase simultaneously, the W content set at 1.5% W and the Co content at 3.8% are preferred, as is consistent with the above experimental results of the steel with 1.5% W and 3.8% Co obtaining the best deformation resistance at 625 °C.

4. Conclusions

Combined effects of Co and W on the deformation resistance of 12Cr heat-resistant steels were investigated. The following conclusions are drawn from this study:

- (1) When Co content is fixed, the steels with 1.5% W are found having the best deformation resistance. When the content of W is fixed, the steels with 3.1% Co mostly possess the best deformation resistance at 575 and 600 °C, but at 625 °C the steels with 3.8% Co obtain the strongest deformation resistance.
- (2) UTS and YS both increase with decreasing temperature. UTS increases with increasing Co content at 575 °C; however, UTS changes little while varying the Co content at 600 and 625 °C, and increases with increasing W content at 625 °C. UTS of 0.85Mo-1.5W-3.1Co steel is slightly higher than 0.85Mo-1.5W-3.8Co steel, but much higher than that of the other steels at 600 and 625 °C. When the W content is lower (0% or 1.5%), YS with 3.1% Co is the highest at 600 °C or 625 °C, while for high W (3%) steel, the more the Co content, the higher the YS is. The results are mostly in accordance with the results based on the analysis of strain-hardening behavior.
- (3) Deformation resistance is related to the initial dislocation density in the steels, which increases with increasing Co content and decreases with increasing W content. The deformation mechanism of the tested steels during high-temperature tensile tests with low strain rate is that of dislocation creep controlled by recovery, which is in accordance with the creep deformation mechanism for creep tests.
- (4) The thermodynamic calculation results indicate that 0.85Mo-1.5W-3.8Co steel obtains the best deformation resistance at 625 °C, which is consistent with the experimental results.
- (5) 0.85Mo-1.5W-3.1Co steel is the optimization of the composition design for 12Cr ferrite heat-resistant steels for 600 °C class USC steam turbine. Furthermore, 0.85Mo-1.5W-3.8Co steel is supposed to be a potential candidate material for 625 °C class steam turbines.

Acknowledgment

This study was supported by a grant from the Scientific Research Innovation Program of Shanghai Educational Committee (No. 09ZZ16).

References

1. F. Masuyama, History of Power Plants and Progress in Heat Resistant Steels, *ISIJ Int.*, 2001, **41**(6), p 612–625
2. K. Marayama, K. Sawada, and J. Koike, Strengthening Mechanisms of Creep Resistant Tempered Martensitic Steel, *ISIJ Int.*, 2001, **41**(6), p 641–653
3. K. Yamada, M. Igarashi, S. Muneki, and F. Abe, Effect of Co Addition on Microstructure in High Cr Ferritic Steels, *ISIJ Int.*, 2003, **43**(9), p 1438–1443
4. Å. Gustafson and J. Ågren, Possible Effect of Co on Coarsening of $M_{23}C_6$ Carbide and Orowan Stress in a 9% Cr Steel, *ISIJ Int.*, 2001, **41**(4), p 356–360
5. L. Helisa, Y. Toda, T. Hara, H. Miyazaki, and F. Abe, Effect of Cobalt on the Microstructure of Tempered Martensitic 9Cr Steel for Ultra-Supercritical Power Plants, *Mater. Sci. Eng. A*, 2009, **510–511**, p 88–94
6. E.V. Rajakovics, Schnellbestimmung des Krieverhaltens von Aluminium-Gusswerkstoffen durch Warm-Kriegzugversuche, *Aluminium*, 1968, **44**, p 679–682
7. H. Olike, Deformation Mechanism Diagrams with the Strain Rate as a Coordinate, *Mater. Sci. Eng.*, 1980, **45**, p 211–215
8. R. Frank, L. Hagn, and H.J. Schuller, Creep Damage and Intention for Prevention, *Proceedings of the International Symposium 'Prediction of Residual Lifetime of Constructions Operating at High Temperature'*, NIL, The Hague, 1977
9. M. Steen, Creep Life Assessment by Low Strain Rate Tensile Testing, *Int. J. Pres. Ves. Piping*, 1983, **14**, p 201–225
10. L. Kaufman, *Computer Calculation of Phase Diagrams*, Academic Press, New York, 1970
11. F. Sun and T.L. Lin, Superplastic Phenomenon in a Large-grain TiAl Alloy, *Scripta Mater.*, 2001, **44**(4), p 665–670
12. P.J. Ennis and A. Czyrska-Filemonowicz, Recent Advances in Creep-resistant Steels for Power Plant Applications, *Sādhanā*, 2003, **28**, p 709–730
13. J. Hald and L. Korcakova, Precipitate Stability in Creep Resistant Ferritic Steels—Experimental Investigations and Modelling, *ISIJ Int.*, 2003, **43**(3), p 420–427
14. K. Miyahara, J.-H. Hwang, and Y. Shimoide, Aging Phenomena before the Precipitation of the Bulky Laves Phase in Fe-10% Cr Ferritic Alloys, *Scr. Metall. Mater.*, 1995, **32**, p 1917–1921